0026-895X/08/7302-359–368$20.00
MOLECULAR PHARMACOLOGY
Copyright © 2008 The American Society for Pharmacology and Experimental Therapeutics
Mol Pharmacol 73:359–368, 2008

Vol. 73, No. 2
39743/3297233
Printed in U.S.A.

A Novel Actin-Binding Domain on Slo1 Calcium-Activated Potassium Channels Is Necessary for Their Expression in the Plasma Membrane

Shengwei Zou, Smita Jha, Eun Young Kim, and Stuart E. Dryer

Department of Biology and Biochemistry, University of Houston, Houston, Texas

Received July 6, 2007; accepted November 7, 2007

ABSTRACT

Large-conductance Ca^{2+}-activated K^+ (BK_{Ca}) channels regulate the physiological properties of many cell types. The gating properties of BK_{Ca} channels are Ca^{2+}-, voltage- and stretch-sensitive, and stretch-sensitive gating of these channels requires interactions with actin microfilaments subjacent to the plasma membrane. Moreover, we have previously shown that trafficking of BK_{Ca} channels to the plasma membrane is associated with processes that alter cytoskeletal dynamics. Here, we show that the Slo1 subunits of BK_{Ca} channels contain a novel cytoplasmic actin-binding domain (ABD) close to the C terminus, considerably downstream from regions of the channel molecule that play a major role in determining channel-gating properties. Binding of actin to the ABD can occur in a binary mixture in the absence of other proteins. Coexpression of a small ABD-green fluorescent protein fusion protein that competes with full-length Slo1 channels for binding to actin markedly suppresses trafficking of full-length Slo1 channels to the plasma membrane. In addition, Slo1 channels containing deletions of the ABD that eliminate actin binding are retained in intracellular pools, and they are not expressed on the cell surface. At least one point mutation within the ABD (L1020A) reduces surface expression of Slo1 channels to approximately 25% of wild type, but it does not cause a marked effect on the gating of point mutant channels that reach the cell surface. These data suggest that Slo1-actin interactions are necessary for normal trafficking of BK_{Ca} channels to the plasma membrane and that the mechanisms of this interaction may be different from those that underlie F-actin and stretch-sensitive gating.

Large-conductance Ca^{2+}-activated K^+ (BK_{Ca}) channels are widely distributed throughout the nervous system. They are both voltage- and Ca^{2+}-dependent, and they contribute to action potential waveforms, the regulation of repetitive firing, and a variety of membrane potential oscillations. BK_{Ca} channels also regulate the physiology of many types of non-neuronal cells. Consequently, the gating and structure of BK_{Ca} channels have been extensively studied (Lu et al., 2006; Lingle, 2007). In addition to regulation by Ca^{2+} and membrane potential, there is an extensive literature indicating that the gating of BK_{Ca} channels is regulated by membrane stretch (Ehrhardt et al., 1996; Huang et al., 2002; Piao et al., 2003; Tian et al., 2006). Stretch sensitivity of smooth muscle BK_{Ca} channels involves interactions with F-actin, because gating is altered in native cells by treatment with agents that alter actin dynamics (Ehrhardt et al., 1996; Piao et al., 2003; Brainard et al., 2005). Moreover, Slo1 channels can coimmunoprecipitate with actin (Brainard et al., 2005), and the cytosolic domains in Slo1 can bind to cortactin, an actin-binding scaffolding protein (Tian et al., 2006). This latter interaction seems to be essential for stretch-induced activation of BK_{Ca} channels, and it occurs in a cytosolic region of the channel close to a domain known to play a role in Ca^{2+}-dependent gating (Krishnamoorthy et al., 2005; Zeng et al., 2005; Tian et al., 2006).

Much less is known about long-term regulation of BK_{Ca} channels. The *Slo1* gene, known as *KCNMA1* in humans, encodes the pore-forming subunits of BK_{Ca} channels, and it is expressed in a large number ($\geq$20) of different splice variants that in many cases exhibit substantially different gating properties (Shipston, 2001). Most variants exhibit high levels of constitutive trafficking to the plasma membrane in heterologous expression systems, but some variants are largely retained in intracellular compartments (Zarei et al., 2001; Wang et al., 2003; Kim et al., 2007b,c; Ma et al., 2007). These

This study was supported in part by National Institutes of Health grant NS32748.

Article, publication date, and citation information can be found at http://molpharm.aspetjournals.org.

doi:10.1124/mol.107.039743.

ABBREVIATIONS: BK_{Ca}, large-conductance Ca^{2+}-activated K^+; Slo1, pore-forming subunit of BK_{Ca} channel; GLUT, glucose transporter; GFP, green fluorescent protein; E9, embryonic day 9; HEK, human embryonic kidney; PBS, phosphate-buffered saline; GST, glutathione transferase; PAGE, polyacrylamide gel electrophoresis; PBST, phosphate-buffered saline with 0.2% Triton X-100; ABD, actin-binding domain.

observations have allowed identification of sequence motifs that play a role in regulating the trafficking of various Slo1 isoforms. These include hydrophobic endoplasmic reticulum export signals and a sorting motif that is required for selective expression of Slo1 on the apical surface of polarized epithelial cells (Kwon and Guggino, 2004; Zarei et al., 2004). More recently, we and others have identified alternatively spliced C-terminal domains that determine the extent of constitutive steady-state surface expression of BK_{Ca} channels in several cell types (Kim et al., 2007b,c; Ma et al., 2007).

The regulated trafficking of Slo1 channels is a physiologically relevant process in the nervous system. For example, ciliary neurons of the developing chick ciliary ganglion retain BK_{Ca} channels in multiple intracellular stores before formation of synapses with target tissues (Dourado and Dryer, 1992; Chae et al., 2005a,b). Stimulation by multiple endogenous growth factors at around the time of synapse formation with target tissues triggers movement of BK_{Ca} channels into the plasma membrane (Dourado and Dryer, 1992; Cameron et al., 1998; Cameron et al., 2001; Chae et al., 2005a,b). The cytoskeleton plays an important role in the regulated and constitutive trafficking of other membrane proteins, including ion channels and other types of transporters. For example, disruption of cortical F-actin dynamics inhibits trafficking of several membrane proteins to the plasma membrane (Kanzaki and Pessin, 2001; Butterworth et al., 2005; Noda and Sasaki, 2006). In some cases, such as with epithelial sodium channels, the channels bind to actin directly (Mazzochi et al., 2006). In other cases, actin interactions are indirect, and they are mediated by scaffolding proteins such as filamin (Petrecca et al., 2000; Sampson et al., 2003). In the insulin-mediated trafficking of the GLUT-4 transporter, actin does not act as either a static barrier or a scaffold. Instead, dynamic changes in actin structure are required for movement of GLUT-4 into the plasma membrane (Kanzaki et al., 2001). Our recent data from developing chick ciliary neurons suggest that growth factors that regulate BK_{Ca} trafficking act on multiple signaling cascades that impinge on cortical actin dynamics (Lhuillier and Dryer, 2002; Chae and Dryer, 2005a,b; Chae et al., 2005a,b).

In the present study, we have examined the role of actin interactions in the trafficking of BK_{Ca} channels. We demonstrate the existence of a novel actin-binding motif in the cytoplasmic C terminus of Slo1 channels. We also show that interactions with this domain are necessary for normal surface expression in the plasma membrane.

Materials and Methods

Plasmids and Antibodies. Expression plasmids pCMV-Myc-VEDEC, pCMV-Myc-QEERL, and pCMV-Myc-EMVYR encoding N-terminal Myc-tagged VEDEC, QEERL, and EMVYR isoforms of Slo1 were provided by Dr. Min Li (Johns Hopkins University, Baltimore, MD). Other plasmids, including pCMV-Myc-QEERL-ΔABD, pcDNA3.1ABD-GFP, pGEXKG-CT1, pGEXKG-CT2, pGEXKG-CT3, pGEXKG-CT3A, pGEXKG-Slo1CT3B, pGEXKG-CT3C, and pGEXKG-CT3D, were constructed by our laboratory using standard methods. The Slo1 point mutations L1020A, D1022A, or L1025A were made from QEERL isoforms of Slo1 using the QuikChange II site-directed mutagenesis kit (Stratagene, La Jolla, CA). To do this, we designed six antiparallel primers carrying the mutant codon for the required substitutions. The vectors containing Slo QEERL cDNA and GST-CT3B were used as templates for the polymerase chain reaction, which was carried out using *Pyrococcus furiosus* polymerase. Incorporation of oligonucleotide primers generates a mutated plasmid containing staggered nicks. The products were treated with DpnI endonuclease, specific for methylated and hemimethylated DNA, which digests the parental DNA template (because DNA originating from *Escherichia coli* is usually dam methylated). The nicked vector DNA carrying the desired mutations was proliferated in *E. coli* JM109-competent cells. The fidelity of all constructs, including point mutants, was confirmed by sequencing. Mouse anti-myc 9B11 (Cell Signaling Technology Inc., Danvers, MA) was used for immunoblot analysis and for confocal microscopy, whereas fluorescein isothiocyanate-conjugated goat anti-myc ab1263 (Abcam, Cambridge, MA) was used only for confocal microscopy. Actin analyses were carried out with a pan-actin antibody, MAB1501 (Chemicon International, Temecula, CA). Immunoblot and confocal analyses of Slo1 were carried out with MAB5228 (Chemicon International).

Coimmunoprecipitation, Immunoblot Analysis, and GST Pull-Down Assays. For coimmunoprecipitation, embryonic day 9 (E9) ciliary ganglion neurons or HEK293T cells were lysed in radioimmunoprecipitation assay buffer containing 1 mM phenylmethylsulfonyl fluoride, and protease inhibitor mixture (Sigma-Aldrich, St. Louis, MO). Cell extracts were incubated in the presence of anti-myc 9B11, anti-Slo1 MAB5228, or IgG (2 μg each), as indicated in the figures, for 4 h at 4°C, followed by the addition of 20 μl of protein A/G agarose (Santa Cruz Biotechnology, Inc., Santa Cruz, CA) for 12 h. Pellets were collected by centrifugation and washed in PBS containing 0.5% Triton X-100. Then, they were boiled for 5 min in 30 μl of Laemmli sample buffer, and 15 μl of each sample was separated by SDS-PAGE on 10% gels. Samples of cell lysates were used as input controls to identify where on the gels that the protein being probed migrated. Proteins were transferred to nitrocellulose filters by wet transfer (1 h) on ice. Blots were blocked for 1 h at room temperature, washed with Tris-buffered saline/Tween 20 buffer, incubated with one of the primary antibodies (anti-actin MAB1501, anti-Slo1 MAB5228, or anti-myc 9B11) overnight at 4°C, washed again with Tris-buffered saline/Tween 20, and then the membrane was incubated with horseradish peroxidase-conjugated secondary antibody (Pierce Biotechnology, Rockford, IL) for 2 h at room temperature. The proteins were visualized using a chemiluminescent substrate (SuperSignal West Pico; Pierce Biotechnology). For GST pull-down assays, GST, GST-CT1, GST-CT2, GST-CT3, GST-CT3A, GST-CT3B, GST-CT3B, GST-CT3C, or GST-CT3D fusion proteins were expressed and extracted from *E. coli* strain BL21, and 50 μg of each fusion protein was separately bound to 10 μl of glutathione-Sepharose 4B beads (GE Healthcare, Little Chalfont, Buckinghamshire, UK) according to the manufacturer's instructions. HEK293T cell lysates (containing 500 μg of protein per sample) were added to the beads, and the samples were incubated overnight at 4°C with gentle rotation. The beads were washed three times with PBS with 0.2% Triton X-100 (PBST), boiled for 5 min in 30 μl of Laemmli sample buffer, and then 15 μl of each sample was separated on 10% SDS-PAGE, transferred to nitrocellulose, and analyzed by immunoblot using anti-actin MAB1501 as described above. In these experiments, the input lanes were cell lysates from nontransfected HEK293T cells. Their purpose was to show the location of actin on the gel. For in vitro binding assays in a binary mixture, glutathione beads carrying GST-CT3A, GST-CT3B, GST-CT3C, GST-CT3D, or GST (20 μg of each) were incubated with purified rabbit skeletal muscle β-actin (Sigma-Aldrich). The input lane contained 5 μg of actin solely to allow visualization of where on the gel that protein migrated. The beads were then washed three times with PBS and eluted with 10 mM glutathione elution buffer. Eluates were separated by 10% SDS-PAGE, transferred to nitrocellulose, and visualized by immunoblot. Protein bands in immunoblots were quantified by densitometry using ImageJ software (http://rsb.info.nih.gov/ij/; National Institutes of Health, Bethesda, MD). All experiments were repeated three to four times, and the error bars represent S.E.M.

Cell Surface Biotinylation Assays and Actin Polymerization Assays. Cell surface biotinylation was carried out by treating

intact HEK293T cells or dissociated embryonic day 9 ciliary ganglion neurons with sulfosuccinimidyl 2-(biotinamido)-ethyl-1,3-dithiopropionates (Pierce Biotechnology) (1 mg/ml in PBS buffer) for 30 min on ice with gentle shaking. Ice-cold PBS buffer containing 100 mM glycine was then added to stop the reaction. After an additional 20 min of incubation, the cells were collected and lysed by gentle trituration in PBS containing 1% Triton X-100. The biotinylated proteins from the cell surface were recovered from the lysates by incubation with immobilized streptavidin-agarose beads (Pierce Biotechnology). Bound proteins were eluted from the beads in Laemmli buffer, and a portion of the original lysate was also saved. Total proteins were then separated on SDS-PAGE and transferred to nitrocellulose; the proteins were quantified by immunoblot. Measurements of the steady-state G-actin/F-actin ratio in E9 ciliary ganglion neurons were carried out using a commercial assay (Cytoskelton Inc., Denver, CO) based on the differential solubility of G-actin and F-actin followed by immunoblot analysis. This assay was carried out according to the manufacturer's instructions and using their reagents. Cells were treated with control medium or 1 nM recombinant transforming growth factor-β1 (R & D Systems, Minneapolis, MN) 12 h before actin analysis. These and all subsequent biochemical experiments were repeated at least three times.

Cell Culture and Staining. Embryonic day 9 ciliary ganglion neurons were dissociated and cultured as described in detail previously (Dourado and Dryer, 1992; Subramony et al., 1996; Cameron et al., 1998). HEK293T cells were grown in Dulbecco's modified Eagle's medium (Sigma-Aldrich) containing 10% heat-inactivated fetal bovine serum at 37°C in a 5% CO_2 incubator. HEK293T cells were transiently transfected using FuGENE 6 (Roche Diagnostics, Indianapolis, IN) in serum-reduced medium (Opti-MEM; Invitrogen, Carlsbad, CA) following the manufacturer's instructions. The DNA concentration of each plasmid in the transfection medium was 1 μg/ml. Cells were used for electrophysiology or biochemistry 48 h after transfection. For immunofluorescence staining, ciliary ganglion neurons or transfected HEK293T cells were washed, fixed in 4% paraformaldehyde for 10 min, permeabilized with PBST, blocked with bovine serum albumin, and then exposed to anti-Slo1 MAB5228 and rhodamine-conjugated phalloidin (GE Healthcare) overnight at 4°C. The cells were washed, treated with fluorescein-conjugated secondary antibody, washed in PBS, and mounted using Vectashield (Vector Laboratories, Burlingame, CA). For confocal analysis of surface expression, intact transfected HEK293T cells were treated with mouse anti-myc 9B11 for 20 min in normal culture medium at 37°C. Cells were then rinsed in PBS, fixed in 4% paraformaldehyde for 10 min, permeabilized with PBST, blocked with bovine serum albumin, and then treated with cyanine 3-conjugated goat anti-mouse and fluorescein-conjugated goat anti-myc ab1263 for 1 to 2 h at room temperature. Cells were then rinsed and mounted in Vectashield. Images were collected on an FV-1000 confocal microscope (Olympus, Tokyo, Japan) using a Plan Apo N 60 $\times$ 1.42 numerical aperture oil immersion objective. Green fluorescence was evoked by excitation at 495 nm, and emission was monitored at 519 nm. Red fluorescence was evoked by excitation at 580 nm, and emission was monitored at 620 nm.

Electrophysiology and Statistics. HEK293T cells were cotransfected with plasmids encoding either GFP or GFP-fusion proteins, along with N-terminal myc-tagged forms of the VEDEC, QEERL, or EMVYR isoforms of Slo1. All physiological recordings were conducted at room temperature. Whole-cell recordings were made from fluorescent HEK293T cells as described previously (Kim et al., 2007c). In brief, the bathing solution contained 150 mM NaCl, 0.08 mM KCl, 0.8 mM $MgCl_2$, 5.4 mM $CaCl_2$, 10 mM glucose, and 10 mM HEPES, and the pH was adjusted to 7.4 with NaOH. The pipette solution contained 145 mM NaCl, 2 mM KCl, 6.2 mM $MgCl_2$, 10 mM HEPES, 5.0 mM H-EDTA, and 5 μM $CaCl_2$, pH 7.2. The free Ca^{2+} concentration in this solution was checked using an Orion 97-20 calcium electrode (Thermo Fisher Scientific, Waltham, MA) calibrated using solution standards obtained from WPI (Sarasota, FL). HEK293T cells do not express endogenous voltage-activated Ca^{2+} currents, and these ionic conditions were chosen to provide sufficient intracellular Ca^{2+} for activation of BK_{Ca} channels by depolarizing step pulses while keeping the resulting macroscopic currents sufficiently small to avoid saturation of the patch-clamp amplifier or significant series resistance errors. To ensure this, the concentration of K^+ ions on both sides of the membrane was reduced 60-fold from physiological, which reduces macroscopic currents but still provides for a physiological K^+ equilibrium potential of -80 mV. Whole-cell currents are not detectable when recording pipettes contain no added $CaCl_2$ and 10 mM EGTA (data not shown). These recording electrodes had resistances of 3 to 4 MÙ, and it was possible to compensate up to 85% of this without introducing oscillations into the current output of the patch-clamp amplifier (Axopatch 1D; Molecular Devices, Sunnyvale, CA). Whole-cell currents were evoked by a series of eight 450-ms depolarizing steps (from -25 to $+80$ mV in 15-mV increments) from a holding potential of -60 mV.

For inside-out patch recordings, pipette solutions contained 150 mM KCl, 0.5 mM $MgCl_2$, 10 mM HEPES, and 5 mM EGTA, pH 7.2. The bath solutions contained 150 mM KCl and 10 mM HEPES, and pH was adjusted to 7.2 after addition of the Ca^{2+} buffer. This consisted of 5 mM EGTA for the Ca^{2+}-free solutions, or 5 mM *N*-hydroxy-EDTA titrated to 20 μM free Ca^{2+} by addition of $CaCl_2$ while monitoring free calcium with the calcium electrode. Patches were excised into Ca^{2+}-free solutions, and then they were switched to the solution containing 20 μM free Ca^{2+}. Currents were evoked in the presence of Ca^{2+} by a series of 250-ms depolarizing voltage pulses from a holding potential of -60 mV. Because K^+ equilibrium potential under these conditions is 0 mV, substantial inward tail currents occur immediately after the break of the depolarizing steps, when patches return to the holding potential. All quantitative data from electrophysiological measurements were analyzed off-line using pCLAMP software (Molecular Devices), and they are presented as mean $\pm$ S.E.M. The data in bar graphs were compiled from 9 to 25 cells in each group. Data were analyzed by one-way analysis of variance followed by post hoc analysis (STATISTICA; Statsoft, Tulsa, OK) using Tukey's honestly significant difference test for unequal sample size, with $p < 0.05$ regarded as significant.

Results

Actin Bound to a Domain on the Cytoplasmic C Terminus of Slo1 Channels. Actin-Slo1 interactions in native neurons were established by coimmunoprecipitation from E9 chick ciliary ganglion extracts. This was observed two ways: with initial precipitation carried out using a commercially available antibody against Slo1, followed by immunoblot with an antibody against actin (Fig. 1A); and also by immunoprecipitation with anti-actin followed by probing of immunoblots with an antibody against Slo1 (Fig. 1B). Confocal microscopy using the same Slo1 antibody reveals that a pool of Slo1 channels close to the plasma membrane colocalizes with rhodamine-conjugated phalloidin, a marker for F-actin (Fig. 1C), which occurs at high levels in cortical regions subjacent to some regions within the plasma membrane. It bears noting that Slo1 signal is markedly reduced on those portions of the neuronal soma surface in which a subjacent layer of cortical actin cannot be detected.

Native neurons present formidable technical limitations for analysis of channel trafficking. Therefore, we have used HEK293T cells to analyze the nature and functional significance of Slo1-actin interactions. We initially expressed three different alternatively spliced variants of mammalian Slo1 channels, and we examined their interactions with actin by coimmunoprecipitation. We have previously referred to these

isoforms as VEDEC, QEERL, and EMVYR, after the last five residues in each variant (Kim et al., 2007b,c). All three Slo1 expression constructs contain an N-terminal (ectofacial) myc tag. Placing a myc tag in this position has previously been shown to have minimal effects on gating and trafficking of BK_{Ca} channels (Meera et al., 1997; Wang et al., 2003). HEK293T cells expressing these channels were lysed, and Slo1 channels were immunoprecipitated, in this case using an antibody against the myc tags. We observed that actin could be detected in the immunoprecipitates of all three Slo1 isoforms by immunoblot analysis using a pan-actin antibody (Fig. 1C). Thus, the interaction between Slo1 and actin can be detected with multiple antibodies that recognize the Slo1 channels.

What portions of the Slo1 molecule bind to actin? To address this question, we prepared a series of GST-fusion proteins including cytoplasmic portions of Slo1, focusing on the C-terminal regions that are conserved in all three variants, starting immediately after the last transmembrane domain (S6) (Fig. 2A). We initially subdivided this large cytoplasmic tail into three components: CT1 (from Glu324 to Pro783), CT2 (from Gly784 to Ala984), and CT3 (from Leu985 to Gln1108). Note that Gln1108 is the last residue conserved in all three Slo1 expression constructs described above. Fixed amounts of these GST-fusion proteins were bound to glutathione-Sepharose 4B beads, which were then added to an extract of nontransfected HEK293T cells. Proteins bound to the beads were eluted, separated by SDS-PAGE, and analyzed by immunoblot. We observed that GST-CT3 could pull actin out of the HEK293T cell lysate but that the GST-CT1 or GST-CT2 constructs, and GST itself, were ineffective (Fig. 2B). Therefore, the CT3 region was further subdivided into four smaller domains, CT3A, CT3B, CT3C, and CT3D (shown schematically in Fig. 2A), which were prepared as GST-fusion proteins. We observed that GST-CT3B could pull actin out of a HEK293T cell lysate but that the other GST-CT3 constructs could not (Fig. 2C, top). The GST pull-down assays described above were performed on a whole-cell lysate, and we cannot exclude that actin interactions with the C-terminal portions of Slo1 are indirect; in other words, such an observation could reflect formation of a larger complex that includes some other actin-binding protein, such as cortactin (Tian et al., 2006), microtubule-associated protein 1A (Park et al., 2004), or filamin A (Kim et al., 2007a). To address this, we observed that GST-CT3B, but not GST or the other GST-fusion proteins, can bind to purified rabbit skeletal muscle actin in a binary mixture in which no other proteins were present (Fig. 2C, bottom). These data indicate that the Slo1-actin interaction is direct and that there is an actin-binding motif somewhere between residues Phe1015 and Thr1049 of the three mammalian Slo1 proteins, a region that has the primary sequence FGIYRLRDAHLSTPSQCTKRYVITNPPY-EFELVPT, hereafter referred to as the actin-binding domain (ABD). It bears noting that Ma et al. (2007) also detected actin binding to a Slo1-GST fusion protein that contained the ABD identified here.

The Actin-Binding Motif on Slo1 Channels Was Required for Expression in the Plasma Membrane. The ABD is close to domains required for endoplasmic reticulum export and trafficking in polarized epithelial cells (Kwon and

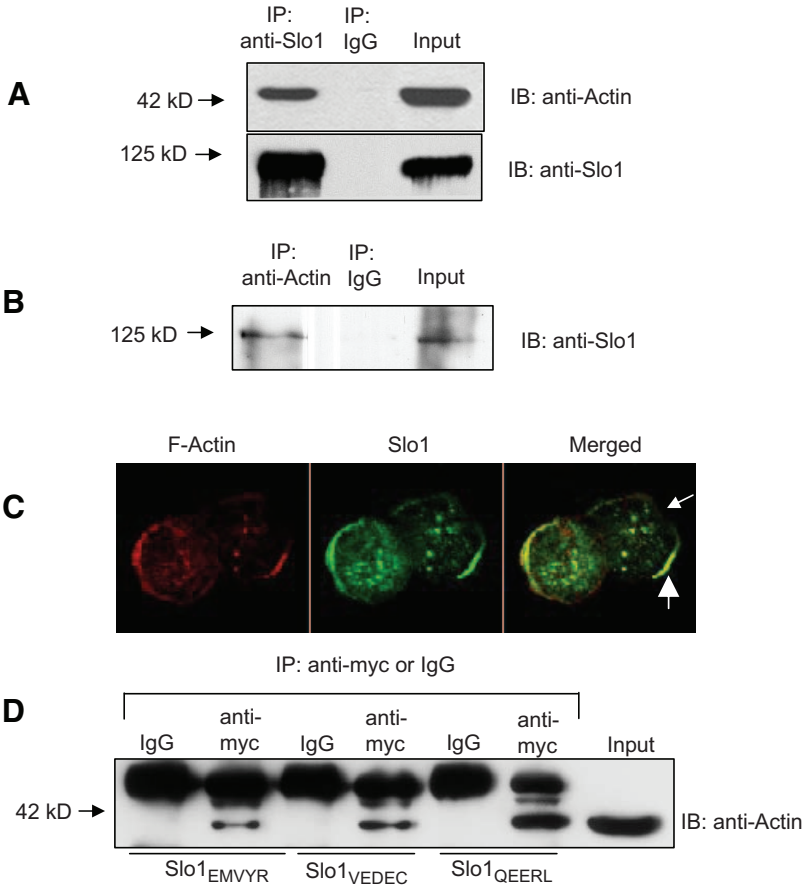

Fig. 1. Interactions between actin and Slo1 channels. A, endogenous actin immunoprecipitates with Slo1 channels in E9 chick ciliary ganglion neurons (top). Immunoblots show proteins that coimmunoprecipitate from neuronal cell lysates using an antibody against Slo1 channels or with IgG, as indicated. The blots were probed with a pan-actin antibody. The blot was then stripped and reprobed with an antibody against Slo1 (middle). Throughout this figure, the lane marked input refers to sample of cell lysates before immunoprecipitation, which serves to demonstrate only the mol. wt. of the protein being probed. B, endogenous Slo1 immunoprecipitates with actin in E9 chick ciliary ganglion neurons. Immunoblots show proteins that coimmunoprecipitate from neuronal cell lysates using an antibody against actin or with IgG, as indicated. C, colocalization of F-actin and Slo1 channels in the soma of E9 ciliary ganglion neurons. F-actin was stained with rhodamine-conjugated phalloidin (red), and Slo1 was localized using the same antibody used in A (green). Regions of colocalization are yellow in the merged image. Large arrow indicates regions of the cell surface where Slo1 and F-actin are both present. Small arrow indicates that Slo1 signal is weak in areas of the cell surface that lack subjacent F-actin. Scale bar, 10 μm. D, coimmunoprecipitation of actin with three different Slo1 splice variants heterologously expressed in HEK293T cells. Immunoprecipitation was carried out with an antibody against the N-terminal myc tags on the Slo1 channels. The splice variants are named according to the five last residues at the C-terminal end. The input lane in this experiment contained a sample of nontransfected HEK293T cell lysate.

Guggino, 2004). Therefore, we hypothesized that the ABD may be involved in channel trafficking to the plasma membrane. This hypothesis makes two specific predictions. First, if direct Slo1 binding to actin is essential for trafficking then it should be possible to perturb surface expression by coexpressing a small molecule that competes with full-length Slo1 channels for actin binding. To test this hypothesis, we coexpressed full-length Slo1 QEERL channels with an ABD-GFP fusion protein in HEK293T cells. We chose to focus on the QEERL isoform because it is expressed in native neurons (Kim et al., 2007b) and because it has a high level of constitutive trafficking to the plasma membrane (Kim et al., 2007b; Ma et al., 2007). In control experiments, we coexpressed the full-length Slo1 channels with GFP. After 24 h, the surface expression of functional cell surface Slo1 channels was assessed by biochemical and electrophysiological methods. In the most direct approach, we observed that coexpression of ABD-GFP markedly reduced surface expression of the Slo1 compared with control cells coexpressing GFP, as assessed by cell surface biotinylation assays in HEK293T cells (Fig. 3, A and B). However, coexpression of ABD-GFP did not effect the total amount of Slo1 expressed compared with cells coexpressing GFP. Addition of the ABD (in the form of GST-CT3B) to a cell lysate reduced the amount of actin that coimmunoprecipitates with myc-tagged Slo1 channels compared with what is observed when GST-CT3A is added to the same lysate (Fig. 3, B and C). Recall that GST-CT3A does not bind actin (Fig. 2C), and this result indicates that the CT3B construct competes with full-length channels for binding to actin. A similar pattern was seen with whole-cell recording. In these experiments, recording electrodes were filled with a saline containing 5 μM free Ca^{2+} so as to allow for robust activation of BK_{Ca} channels in HEK293T cells by step commands within a range comparable with that observed in excised patches. A more detailed analysis of macroscopic currents observed using these methods has been presented elsewhere (Kim et al., 2007a,b,c), and representative current traces are shown in Fig. 4A. Currents were evoked by depolarizing voltage steps from a holding potential of −60 mV. We observed that coexpression of the ABD-GFP fusion protein resulted in a marked reduction in mean whole-cell currents carried by Slo1 channels compared with those observed when full-length Slo1 subunits were coexpressed with GFP (Fig. 4B). These results collectively indicate that soluble fusion proteins containing the ABD compete with full-length Slo1 channels for access to actin, resulting in reduced steady-state expression in the plasma membrane.

The hypothesis further predicts that removing the ABD from Slo1 channels should block their expression on the cell surface. To test this, we prepared a deletion construct of the QEERL isoform of Slo1 in which 25 residues (Leu1020–Phe1045) within the ABD are removed (Slo1-ΔABD). The Slo1-ΔABD construct contains the same N-terminal myc tag as the full-length Slo1 constructs described above. These constructs were expressed in HEK293T cells, and surface expression was determined using four independent methods of analysis. First, we separately labeled surface and intracellular pools of Slo1 channels for visualization by confocal microscopy. Transfected HEK293T cells were exposed to mouse anti-myc before fixation. Cells were then fixed, permeabilized, and labeled with cyanine 3-conjugated goat anti-mouse and fluorescein isothiocyanate-conjugated goat anti-myc to identify surface and intracellular pools of channels in the same cells (Fig. 5A). We observed full-length Slo1 channels expressed on the cell surface (red fluorescence), along with a pool of channels in intracellular stores (green fluorescence). By contrast, Slo1-ΔABD channels seemed to be completely excluded from the cell membrane, but they were easily detected in intracellular compartments (Fig. 5A). Cell surface biotinylation assays also show that the myc tag on

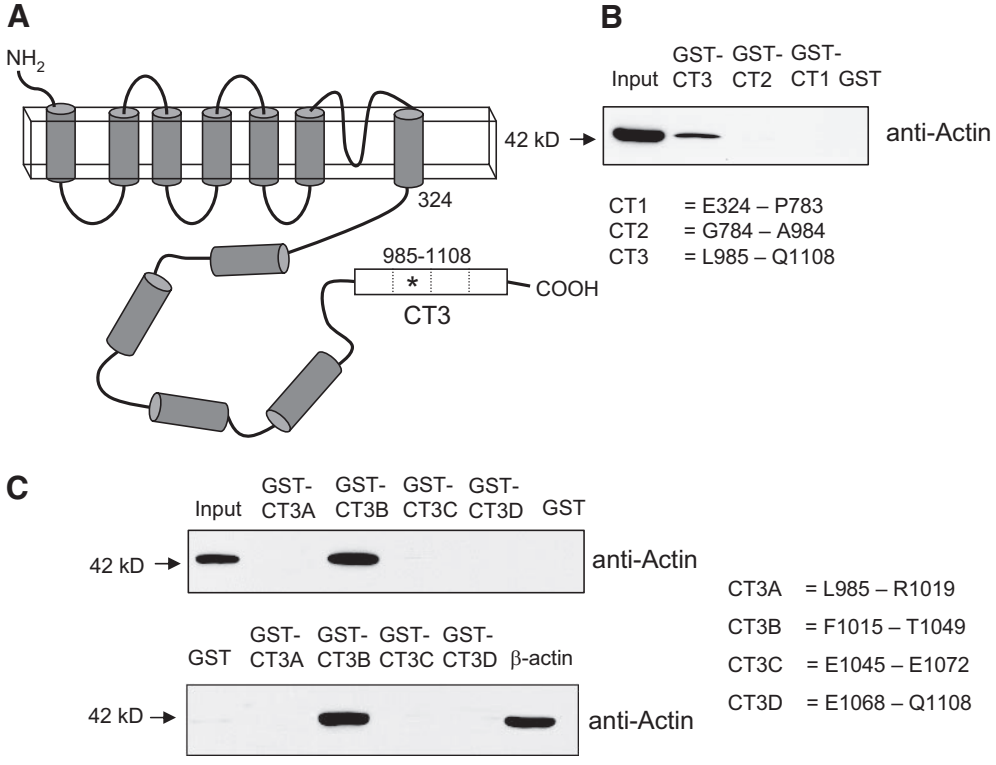

Fig. 2. Interaction of actin with C-terminal domains of Slo1. A, schematic diagram of Slo1 channels. Asterisk indicates location of ABD. B, results of GST pull-down assay carried out on HEK293T cell lysates showing that a GST-CT3 fusion protein binds to actin but that GST-CT2 and GST-CT1 do not. The Slo1 residues that mark the beginning and end of each fusion protein are shown below the blot. These residues are conserved in all three C-terminal variants shown in Fig. 1C. The lane marked input contains a sample of nontransfected HEK293T cell lysate that was not exposed to fusion proteins. It is included only to demonstrate the location of the actin signal on the gel. C, the CT3 domain was further subdivided into four smaller pieces that were prepared as GST-fusion proteins. GST-CT3B binds to actin in HEK293T cell extracts (blot on top) and in binary mixtures with rabbit skeletal muscle actin (bottom), whereas the other constructs do not. The input lane in the top blot contains a sample of HEK293T cell lysate. A control lane in the bottom lane contained 5 μg of purified β-actin to establish where it runs on the gel. Residues of Slo1 included in each of these constructs are indicated adjacent to the immunoblots.

full-length Slo1 channels can be detected on the surface of transiently transfected HEK293T cells, whereas myc tags were below the level of detection on the surface of HEK293T cells expressing Slo1-ΔABD (Fig. 5B). It also bears noting that Slo1-ΔABD channels do not colocalize with F-actin in HEK293T cells, whereas full-length Slo1 channels show extensive colocalization with F-actin as indicated by staining with rhodamine-conjugated phalloidin (Fig. 5C).

In addition, using methods already described, we observed voltage-evoked outward whole-cell currents in HEK293T cells expressing myc-tagged Slo1 channels, but we could not detect whole-cell currents in any cells expressing myc-tagged Slo1-ΔABD (Fig. 6A). It bears noting that cell samples were transfected with the same amounts of DNA for both constructs in all of these experiments, and comparable amounts of both proteins were detected in cell lysates (Fig. 6B). This suggests that the Slo1-ΔABD protein is not subjected to a substantially greater rate of degradation than the full-length Slo1 protein. To further ascertain that functional channels were not being expressed on the cell surface, we also examined currents in excised inside-out patches, measuring currents evoked at +60 mV while the cytoplasmic face of the patch membranes are exposed to 20 μM bath Ca^{2+}. We observed a similar pattern, namely, that virtually no current was detected in patches excised from cells expressing the Slo1-ΔABD construct but that very large (5- to 10-nA) currents were observed in patches excised from cells expressing wild-type Slo1 (Fig. 6B).

The ABD region of Slo1 does not exhibit close homology with the actin-binding regions of other proteins. However, we did notice that the actin-binding regions of some other proteins (Vandekerckhove et al., 1989; Bresnick et al., 1990) contain a degenerate motif that can be described as L/I-*X*-D/E-*X*-*X*-L/I, where *X* can be any residue, and that this motif is found within the Slo1 ABD. To test the hypothesis that these residues contribute in some way to Slo1-actin interactions, we prepared soluble GST-C3B fusion proteins in which residues Leu1020, Asp1022, or Leu1025 of QEERL channels were mutated to alanine, and then we examined whether these proteins could bind to purified β-actin using a GST pull-down assay in a binary mixture. The methods used in this assay were the same as those used in Fig. 2C. We observed that the L1020A mutation caused a reduction in the binding of the resulting GST-fusion protein to purified β-actin but that binding to the D1022A and L1025A mutations was only slightly reduced from wild type (CT3B) (Fig. 7A). To determine the functional effects of these mutations, we prepared expression constructs in which the Leu1020, Asp1022, or Leu1025 residues within full-length Slo1 (QEERL) channels were mutated to alanine, and we examined whether the resulting channels exhibited normal expression on the cell surface using a cell surface biotinylation assay. We observed reduced surface expression of the myc tags of Slo1L1020A channels in HEK293T cells compared with wild-type Slo1 or the Slo1D1022A or Slo1L1025A mutations (Fig. 7B). Total expression was not affected by these point mutations. Consistent with this, expression of full-length Slo1L1020A resulted in currents significantly smaller than wild type in inside-out patches exposed to 20 μM Ca^{2+} at +60 mV, whereas currents carried by Slo1D1022A and Slo1L1025A were indistinguishable from wild-type Slo1 channels (Fig. 8, A and B). The same pattern was also observed in whole-cell recordings in which recording pipettes contained 5 μM Ca^{2+} (Fig. 8, C and D). Unlike the ABD deletion mutants, however, the resulting currents were reduced but not eliminated. The effects of point mutations within the ABD provide an additional line of evidence suggesting that direct binding to actin filaments is necessary for normal steady-state surface expression of Slo1 channel proteins.

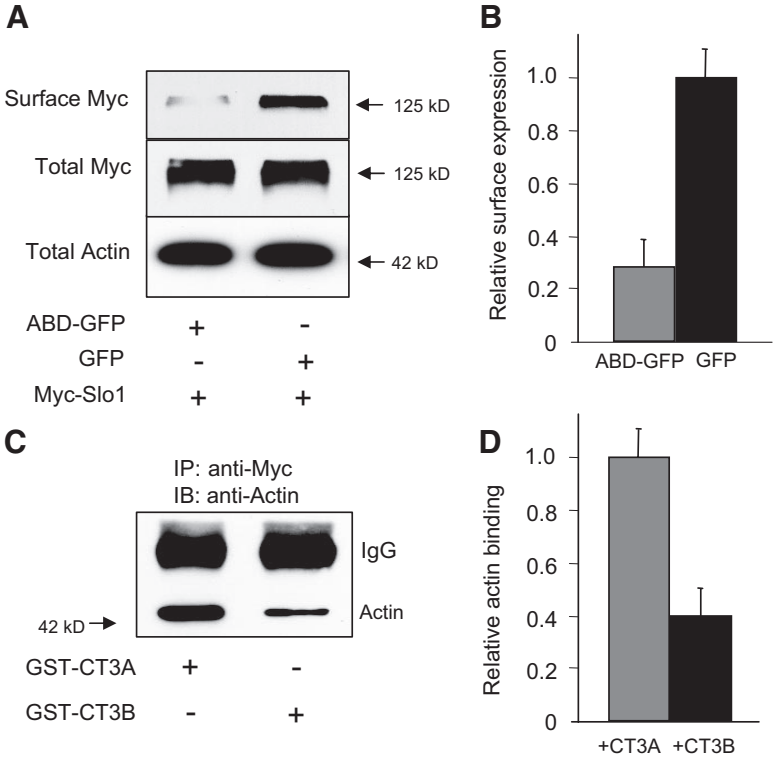

Fig. 3. Coexpression of an ABD-GFP fusion protein reduces surface expression of Slo1 channels in HEK293T cells. The cells were transiently transfected with an expression construct encoding myc-tagged mammalian Slo1 (QEERL isoform), along with ABD-GFP or GFP, as indicated. A, representative cell surface biotinylation assay carried out using antibodies against the ectofacial myc tag present on Slo1. The large arrow indicates 125 kDa; the small arrow indicates 42 kDa. B, densitometric analysis of three replications of the experiment shown in A showing reduction in surface expression in cells expressing ABD-GFP. Data presented are mean ± S.E.M. C, adding purified GST-CT3B to lysates of HEK293T cells expressing myc-tagged Slo1 channels reduces the amount of actin that coimmunoprecipitates with Slo1 channels, indicating competition with Slo1 for binding to actin. This reduction is compared with signal from the same lysates containing an identical amount of GST-CT3A, which does not contain an ABD. Densitometric quantification of three replications of this experiment is shown in D.

Discussion

Actin filaments affect the gating properties of BK_{Ca} channels (Ehrhardt et al., 1996; Huang et al., 2002; Piao et al., 2003; Brainard et al., 2005), and this is thought to underlie the stretch-sensitive gating of these channels. The mechanisms whereby F-actin effects BK_{Ca} gating are not well understood, but recent studies suggest that they entail interactions with actin-binding adaptor proteins that interact with BK_{Ca} channels close to known calcium-binding domains (Tian et al., 2006). Here, we have shown that the pore-forming subunits of BK_{Ca} channels contain a novel ABD that is located in the distal end of the cytoplasmic C terminus, in regions that have not been implicated in regulation of Ca^{2+} binding or channel gating. Actin binding to this ABD of Slo1 channels can occur in vitro in a binary mixture in which no other proteins are present.

These results suggest a model in which F-actin provides an obligatory pathway for Slo1 movement to the cell membrane. We further propose that growth factors alter actin dynamics so as to facilitate movement along these filaments. The final steps of channel insertion into the plasma membrane most likely require the channels to unload from the subjacent actin filaments, possibly by localized F-actin depolymerization, or, alternatively, by binding of other adaptor proteins. If this F-actin unbinding step were to be rate limiting, then cortical actin could function as a barrier to Slo1 insertion into the plasma membrane that is removed upon activation of appropriate growth factor signaling cascades. A very similar model has been proposed for hormone-induced trafficking of GLUT-4 transporters (Kanzaki and Pessin, 2001) and aquaporin channels (Noda and Sasaki, 2006), and we have presented earlier evidence that actin can function as a barrier to insertion of Slo1 channels to the plasma membrane of ciliary ganglion neurons (Chae and Dryer, 2005b).

Slo1 interactions with cortical F-actin seem to resume in at least some systems after membrane insertion, and these interactions contribute to the stretch-sensitivity of BK_{Ca} channels observed in many preparations (Huang et al., 2002; Piao et al., 2003; Tian et al., 2006). This may be indirectly mediated by actin-binding adaptor proteins such as cortactin (Tian et al., 2006), microtubule-associated protein-1A (Park et al., 2004), or filamin A (Kim et al., 2007a). In this regard,

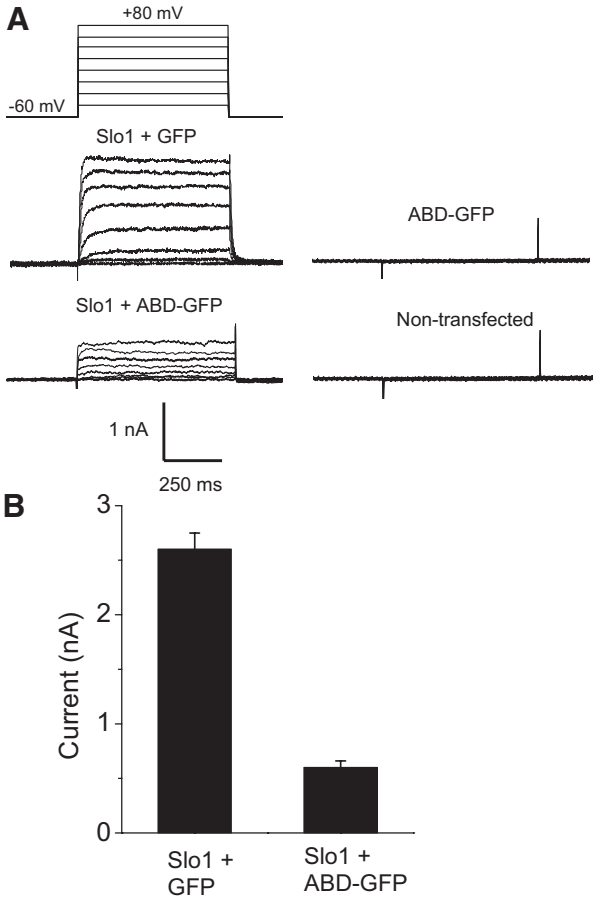

Fig. 4. Coexpression of an ABD-GFP fusion protein reduces expression of functional Slo1 channels. The QEERL isoform of Slo1 channels was coexpressed in HEK293T cells with ABD-GFP or GFP as indicated, and current was then quantified by whole-cell recordings from fluorescent cells. A, representative families of currents evoked by depolarizing voltage steps (shown above traces) in cells coexpressing Slo1 and GFP or Slo1 and ABD-GFP, from a cell expressing only ABD-GFP, and from a non-transfected cell. The recording electrodes were filled with a saline containing 5 μM free Ca^{2+} to allow for activation of the channels. Additional characteristics of these macroscopic currents are provided in Kim et al. (2007a). B, mean ± S.E.M. of the maximal currents (at +60 mV) from cells coexpressing Slo1 with GFP or ADP-GFP.

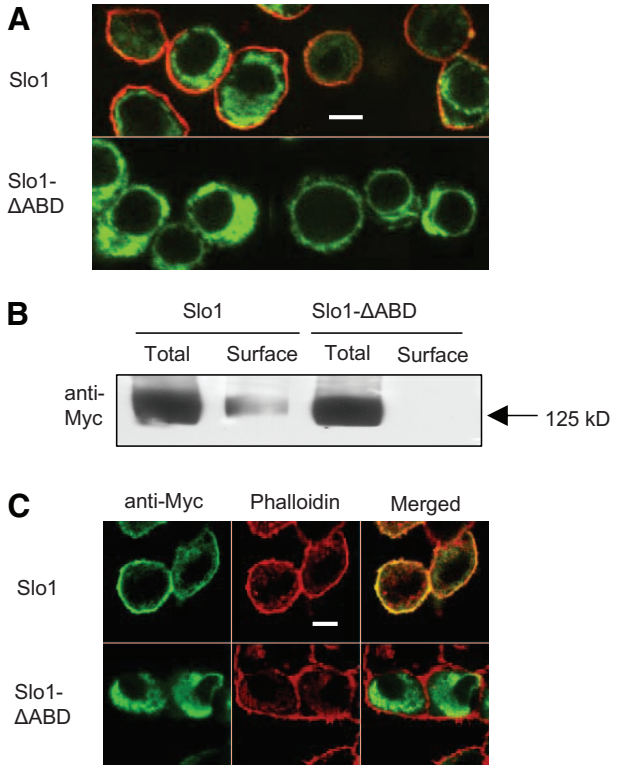

Fig. 5. The ABD is necessary for expression of Slo1 channels in the plasma membrane. These data are from HEK293T cells expressing the full-length QEERL isoform of Slo1, or a deletion mutant missing 25 residues within the ABD (Slo1-ΔABD). A, confocal immunofluorescence using antibodies against the ectofacial myc tags present in both constructs. Surface channels labeled in intact cells fluoresce red, whereas channels that can be detected after fixation and membrane permeabilization fluoresce green. B, a similar pattern is observed by cell surface biotinylation assays using antibodies against the myc tag on the Slo1 channels. C, Slo1-ΔABD expressed in HEK293T cells (green fluorescence from the myc tag) does not colocalize with F-actin stained with rhodamine-conjugated phalloidin (red fluorescence), whereas wild-type Slo1 channels show extensive colocalization that is easily seen in merged images as a yellow signal. Scale bars, 10 μm.

we have recently shown that the actin-binding protein filamin A, which forms cross-links between perpendicularly oriented actin filaments, binds to the cytoplasmic C terminus of BK_{Ca} channels, leading to an increase in the steady-state surface expression of these channels (Kim et al., 2007a). A surprising feature of this effect is that it persists when BK_{Ca} channels interact with filamin A deletion mutants that lack their actin-binding domains. The fact that BK_{Ca} channels bind directly to actin can explain some of these observations.

Do direct actin interactions affect other aspects of BK_{Ca} function? We cannot exclude that the ABD contributes to stretch-sensitive gating because the ABD is located on cytoplasmic domains in the C terminus. We are experimentally limited by the fact that complete inhibition of actin binding seems to prevent surface expression, which precludes making the necessary recordings. However, it is worth noting that the ABD in Slo1 channels is located considerably downstream of the regulator of conductance of K^+ channels domain and calcium bowl domain that are thought to comprise the Ca^{2+}-binding sites that mediate most physiological gating processes of these channels (Krishnamoorthy et al., 2005; Zeng et al., 2005). The ABD is also located at some distance from a pair of noncanonical C-terminal Src homology 3 domains that are involved in stretch-sensitive gating (Tian et al., 2006). Instead, the ABD is almost adjacent to motifs required for endoplasmic reticulum export (DLIFCL) and selective expression on the apical surface of polarized epithelial cells (NAGQSRA) (Kwon and Guggino, 2004). This suggests that the distal C-terminal portions of Slo1 channels that include the ABD play a greater role in channel trafficking or localization within membrane domains than in channel gating.

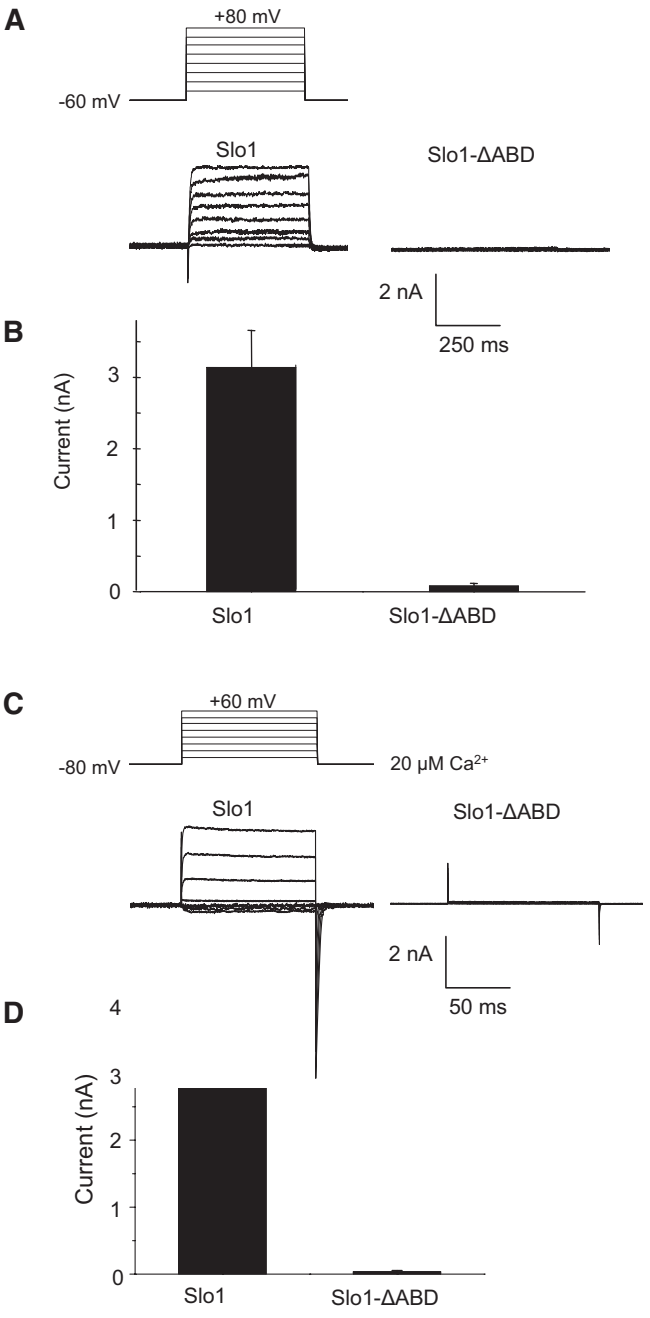

Fig. 6. The ABD is necessary to detect functional Slo1 channels in the plasma membrane of HEK293T cells. A, whole-cell recordings showing families of currents in cells expressing full-length Slo1 channels or Slo1-ΔABD channels, as indicated. The voltage-clamp protocol is shown above the Slo1 current traces. B, summary of results showing mean ± S.E.M. of maximal currents evoked by depolarizing steps to +60 mV in 14 cells in each group. Note absence of whole-cell currents in HEK293T cells expressing Slo1-ΔABD. C, similar pattern is observed in excised inside-out patch recordings from HEK293T cells expressing the same constructs. The traces are representative families of currents evoked by a series of step voltage pulses in inside-out patches exposed to 20 μM free Ca^{2+} in the bath solution, shown above the Slo1 traces. Recordings in this case were made in symmetrical KCl, leading to large tail currents in patches expressing Slo1. D, summary of results from 10 inside-out patches in each group showing mean ± S.E.M. of maximal currents evoked by depolarizing steps to +60 mV in the presence of 20 μM free Ca^{2+}.

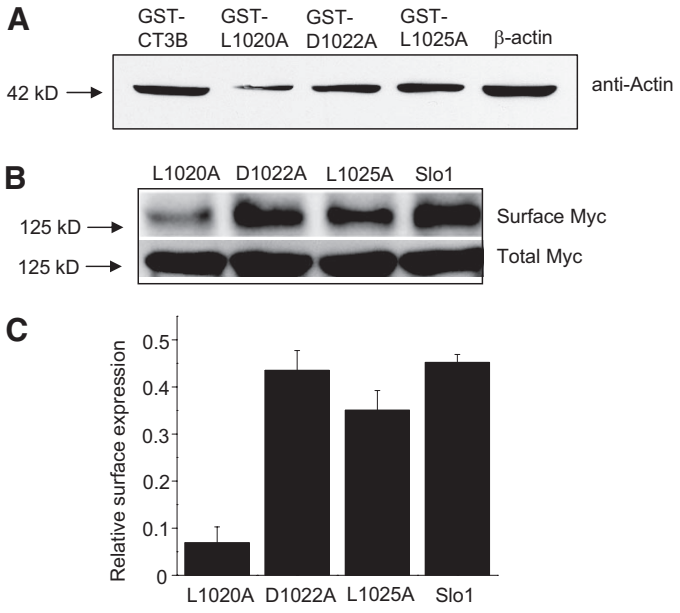

Fig. 7. A point mutation within the ABD affects Slo1 binding to purified actin and its surface expression in HEK293T cells. A, GST pull-down assays carried out against purified β-actin. The GST-Slo1 fusion proteins used in these assays consisted of wild-type GST-CT3B, and three other corresponding fusion proteins in which Leu1020, Asp1022, or Leu1025 were mutated to alanine, as indicated. Note reduced actin binding to the L1020A mutant, whereas the other two point mutations showed binding indistinguishable from wild-type GST-CT3B. A control lane was loaded with purified β-actin to show where it runs on the gel. B, cell-surface biotinylation assay of full-length wild-type Slo1 channels (QEERL isoform) and corresponding channels containing the L1020A, D1022A, or L1025A mutations, as indicated. Densitometric quantification of three replications of this experiment is shown in D.

One question that arises is whether the ABD in Slo1 channels is similar to the actin-binding motifs of other proteins. Searches of databases have not revealed long stretches of obvious homology between this domain and anything else. However, a series of six residues within the Slo1 ABD (LRDAHL) contain a highly degenerate motif, L/I-*X*-D/E-*X*-*X*-L/I, that we have noticed within the established actin-binding domains of at least two other proteins, including ABP-120 (LVDKNL) (Bresnick et al., 1990) and profilin (LADYLI) (Vandekerckhove et al., 1989). These are obviously highly degenerate sequences that would be expected to occur by chance in many proteins. We observed that mutating the first lysine in this motif to alanine reduced Slo1-actin interactions and caused a marked reduction in trafficking of the resulting channels to the plasma membrane. However, mutating the glutamate or the second lysine residue in this motif to alanine did not affect Slo1 trafficking, and it did not substantially affect actin binding, suggesting that the presence of this motif in multiple actin-binding proteins may have occurred by chance. Fortuitously, these data provide another line of evidence that a region within the Slo1 ABD contributes to direct and functionally significant interactions with cytoskeletal elements that are necessary for normal expression of these channels on the cell surface.

In summary, we have identified a novel actin-binding domain in the distal cytoplasmic tail of the principal subunits of large-conductance BK_{Ca} channels that contributes to regulation of the normal steady-state expression of these channels on the plasma membrane. It is possible that dynamic changes in the actin cytoskeleton are required for growth factor-evoked increases in surface expression of neuronal BK_{Ca} channels.

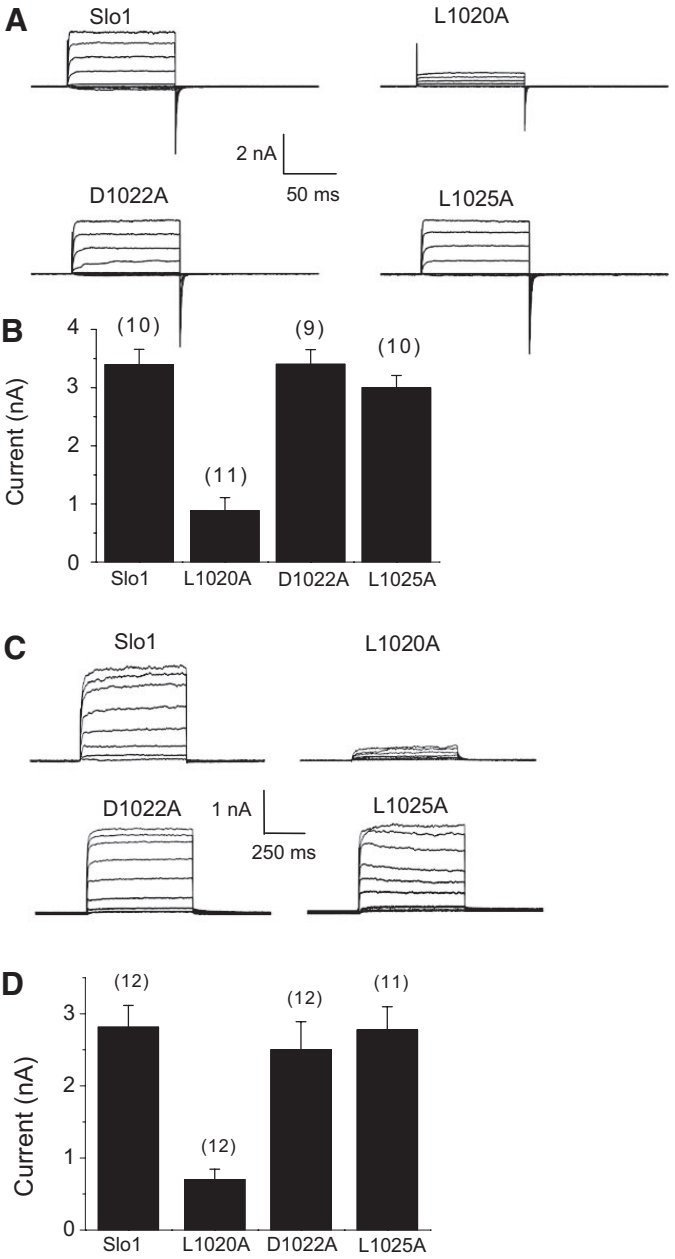

Fig. 8. A point mutation within the ABD reduces the amplitude of macroscopic currents. A, representative families of currents in inside-out recordings from HEK293T cells obtained in the presence of 20 μM free Ca^{2+} in the bath. Recordings were made using the protocols shown in Fig. 6B. Note reduced but detectable currents in cells expressing the L1020A mutant compared with those observed in cells expressing wild-type Slo1 or the other mutants. B, summary of results from several patches in each group. Data are mean ± S.E.M., and the numbers in parentheses are the number of patches analyzed in each group. C, families of typical whole-cell currents evoked using the protocols shown in Fig. 6A. D, plot of mean currents ± S.E.M., with the number of cells in each group is indicated in parentheses.

Acknowledgments

We are grateful to Dr. Min Li for the myc-tagged Slo1 expression constructs.

References

Brainard AM, Miller AJ, Martens JR, and England SK (2005) Maxi-K channels localize to caveolae in human myometrium: a role for an actin-channel-caveolin complex in the regulation of myometrial smooth muscle K^+ current. *Am J Physiol Cell Physiol* **289:**C49–C57.

Bresnick AR, Warren V, and Condeelis J (1990) Identification of a short sequence essential for actin binding by *Dictyostelium* ABP-120. *J Biol Chem* **265:**9236–9240.

Butterworth MB, Frizzell RA, Johnson JP, Peters KW, and Edinger RS (2005) PKA-dependent ENaC trafficking requires the SNARE-binding protein complexin. *Am J Physiol Renal Physiol* **289:**F969–F977.

Cameron JS, Dryer L, and Dryer SE (2001) β-Neuregulin-1 is required for the in vivo development of functional Ca^{2+}-activated K^+ channels in parasympathetic neurons. *Proc Natl Acad Sci U S A* **98:**2832–2836.

Cameron JS, Lhuillier L, Subramony P, and Dryer SE (1998) Developmental regulation of neuronal K^+ channels by target-derived TGFβ in vivo and in vitro. *Neuron* **21:**1045–1053.

Chae KS and Dryer SE (2005a) Regulation of neuronal K_{Ca} channels by β-neuregulin-1 does not require activation of Ras-MEK-extracellular signal-regulated kinase signaling cascades. *Neuroscience* **135:**1013–1016.

Chae KS and Dryer SE (2005b) The p38 mitogen-activated protein kinase pathway negatively regulates Ca^{2+}-activated K^+ channel trafficking in developing parasympathetic neurons. *J Neurochem* **94:**367–379.

Chae KS, Martin-Caraballo M, Anderson M, and Dryer SE (2005a) Akt activation is necessary for growth factor-induced trafficking of functional K_{Ca} channels in developing parasympathetic neurons. *J Neurophysiol* **93:**1174–1182.

Chae KS, Oh KS, and Dryer SE (2005b) Growth factors mobilize multiple pools of K_{Ca} channels in developing parasympathetic neurons: role of ADP-ribosylation factors and related proteins. *J Neurophysiol* **94:**1597–1605.

Dourado MM and Dryer SE (1992) Changes in the electrical properties of chick ciliary ganglion neurones during embryonic development. *J Physiol* **449:**411–428.

Ehrhardt AG, Frankish N, and Isenberg G (1996) A large-conductance K^+ channel that is inhibited by the cytoskeleton in the smooth muscle cell line DDT1 MF-2. *J Physiol* **496:**663–676.

Huang H, Rao Y, Sun P, and Gong LW (2002) Involvement of actin cytoskeleton in modulation of Ca^{2+}-activated K^+ channels from rat hippocampal CA1 pyramidal neurons. *Neurosci Lett* **332:**141–145.

Kanzaki M and Pessin JE (2001) Insulin-stimulated GLUT4 translocation in adipocytes is dependent upon cortical actin remodeling. *J Biol Chem* **276:**42436–42444.

Kim EY, Ridgway LD, and Dryer SE (2007a) Interactions with filamin A stimulate surface expression of large conductance Ca^{2+}-activated K^+ channels in the absence of direct actin binding. *Mol Pharmacol* **72:**622–630.

Kim EY, Ridgway LD, Zou S, Chiu YH, and Dryer SE (2007b) Alternatively spliced C-terminal domains regulate the surface expression of large conductance calcium-activated potassium channels. *Neuroscience* **146:**1652–1661.

Kim EY, Zou S, Ridgway LD, and Dryer SE (2007c) β1-subunits increase surface

expression of a large-conductance Ca^{2+}-activated K^+ channel isoform. *J Neurophysiol* **97:**3508–3516.
Krishnamoorthy G, Shi J, Sept D, and Cui J (2005) The NH_2 terminus of RCK1 domain regulates Ca^{2+}-dependent BK_{Ca} channel gating. *J Gen Physiol* **126:**227–241.
Kwon SH and Guggino WB (2004) Multiple sequences in the C terminus of MaxiK channels are involved in expression, movement to the cell surface, and apical localization. *Proc Natl Acad Sci U S A* **101:**15237–15242.
Lhuillier L and Dryer SE (2002) Developmental regulation of neuronal K_{Ca} channels by TGFβ1: an essential role for PI3 kinase signaling and membrane insertion. *J Neurophysiol* **88:**954–964.
Lingle CJ (2007) Gating rings formed by RCK domains: keys to gate opening. *J Gen Physiol* **129:**101–107.
Lu R, Alioua A, Kumar Y, Eghbali M, Sefani E, and Toro L (2006) MaxiK channel partners: physiological impact. *J Physiol* **570:**65–72.
Ma D, Nakata T, Zhang G, Hoshi T, Li M, and Shikano S (2007) Differential trafficking of carboxyl isoforms of Ca^{2+}-gated (Slo1) potassium channels. *FEBS Lett* **581:**1000–1008.
Mazzochi C, Bubien JK, Smith PR, and Benos DJ (2006) The carboxyl terminus of the alpha-subunit of the amiloride-sensitive epithelial sodium channel binds to F-actin. *J Biol Chem* **281:**6528–6538.
Meera P, Wallner M, Song M, and Toro L (1997) Large conductance voltage- and calcium-dependent K^+ channel, a distinct member of voltage-dependent ion channels with seven N-terminal transmembrane segments (S0–S6), an extracellular N terminus, and an intracellular (S9–S10) C terminus. *Proc Natl Acad Sci U S A* **94:**14066–14071.
Noda Y and Sasaki S (2006) Regulation of aquaporin-2 trafficking and its binding protein complex. *Biochem Biophys Acta* **1758:**1117–1125.
Park SM, Liu G, Kubal A, Fury M, Cao L, and Marx SO (2004) Direct interaction between BK_{Ca} potassium channel and microtubule-associated protein 1A. *FEBS Lett* **570:**143–148.
Petrecca K, Miller DM, and Shrier A (2000) Localization and enhanced current density of the Kv4.2 potassium channel by interaction with the actin-binding protein filamin. *J Neurosci* **20:**8736–8744.
Piao L, Ho WK, and Earm YE (2003) Actin filaments regulate the stretch sensitivity of large-conductance, Ca^{2+}-activated K^+ channels in coronary artery smooth muscle cells. *Pflugers Arch* **446:**523–528.
Sampson LJ, Leyland ML, and Dart C (2003) Direct interaction between the actin-binding protein filamin-A and the inwardly rectifying potassium channel, Kir2.1. *J Biol Chem* **278:**41988–41997.
Shipston MJ (2001) Alternative splicing of potassium channels: a dynamic switch of cellular excitability. *Trends Cell Biol* **11:**353–358.
Subramony P, Raucher S, Dryer L, and Dryer SE (1996) Posttranslational regulation of Ca^{2+}-activated K^+ currents by a target-derived factor in developing parasympathetic neurons. *Neuron* **17:**115–124.
Tian L, Chen L, McClafferty H, Sailer CA, Ruth P, Knaus HG, and Shipston MJ (2006) A noncanonical SH3 domain binding motif links BK channels to the actin cytoskeleton via the SH3 adapter cortactin. *FASEB J* **20:**2588–2590.
Vandekerckhove JS, Kaiser DA, and Pollard TD (1989) Acanthamoeba actin and profilin can be cross-linked between glutamic acid 364 of actin and lysine 115 of profilin. *J Cell Biol* **109:**619–626.
Wang SX, Ikeda M, and Guggino WB (2003) The cytoplasmic tail of large conductance, voltage- and Ca^{2+}-activated K^+ (MaxiK) channel is necessary for its cell surface expression. *J Biol Chem* **278:**2713–2722.
Zarei MM, Eghbali M, Alioua A, Song M, Knaus HG, Stefani E, and Toro L (2004) An endoplasmic reticulum trafficking signal prevents surface expression of a voltage- and Ca^{2+}-activated K^+ channel splice variant. *Proc Natl Acad Sci U S A* **101:**10072–10077.
Zarei MM, Zhu N, Alioua A, Eghbali M, Stefani E, and Toro L (2001) A novel MaxiK splice variant exhibits dominant-negative properties for surface expression. *J Biol Chem* **276:**16232–16239.
Zeng XH, Xia XM, and Lingle CJ (2005) Divalent cation sensitivity of BK channel activation supports the existence of three distinct binding sites. *J Gen Physiol* **125:**273–286.

Address correspondence to: Dr. Stuart E. Dryer, Department of Biology and Biochemistry, University of Houston, 4800 Calhoun, Houston, TX 77204-5001. E-mail: sdryer@uh.edu